Sum Frequency Generation Investigation of Glycerol/Water Surfaces

Steve Baldelli, Cheryl Schnitzer, and Mary Jane Shultz*

Department of Chemistry, Tufts University, Medford, Massachusetts 02155

D. J. Campbell

Department of Chemistry, College of the Holy Cross, Worcester, Massachusetts 01610

Received: November 19, 1996; In Final Form: April 10, 1997[⊗]

The OH and CH regions of glycerol/water mixtures in the concentration range 0.0−1.0 mole fraction have been investigated with vibrational sum frequency generation. Glycerol is found to partition to the surface of these solutions in all concentrations. Neat glycerol surfaces contain no free OH groups projecting into the vapor. The surface orientation of glycerol is constant through most of the concentration range.

Introduction

The surfaces of neat liquids and mixtures have been of interest for almost a century.[1] Unfortunately, obtaining bonding and orientation information for molecules at this interface has been experimentally difficult[2] due to the lack of a probe capable of detecting molecular details at pressures near an atmosphere. Understanding these details, however, is crucial to numerous fields including developing mechanisms of heterogeneous catalysis in the environment. In the last decade, this situation has changed with infrared−visible sum frequency generation (SFG) being used to study neat liquid/vapor interfaces[3,4] and the liquid/vapor interface of mixtures of two mutually soluble liquids.[5,6] In the study of two miscible liquids, SFG has been used to determine surface coverage and orientation of the organic component. In methanol/water[5] and acetonitrile/water[6] mixtures, it is found that the organic component partitions to the surface and is oriented with its polar end toward the bulk. Further, these organic molecules form an ordered structure at the air/liquid interface at a specific concentration.

In this paper, we report the results of an SFG investigation of the energetics and surface partitioning for water/glycerol mixtures having compositions of 0.0-1.0 mole fraction (x) glycerol. Glycerol is observed to partition to the surface of these mixtures. In addition, the SFG spectra indicate that the orientation of glycerol is nearly constant in the range 0.1−1.0x glycerol. To obtain a specific view of hydrogen bonding on the surface, OH groups are probed. It is observed that the free OH peak of water decreases as glycerol is added to water. Free OH refers to an OH group projecting out of the surface, free of hydrogen bonding so that it is more like the hydroxyl in a gas phase molecule. The free OH of water disappears at 0.25x glycerol. In contrast to water, our results indicate that glycerol shows no free OH at any concentration.

Background

SFG is an ideal technique to probe air/liquid interfaces. In the electric dipole approximation, SFG, a $\chi^{(2)}$ process, is forbidden in bulk media but allowed at the surface where inversion symmetry is broken. Hence, SFG is a surface specific technique. As a result of this surface specificity SFG is sensitive to a few hundredths of a monolayer. This type of surface sensitivity and specificity is ideal for studying molecular orientation and concentration at the surface of mixed component systems.

Surface SFG is described extensively in the literature;[4,7−15] hence only essential details are given here. SFG arises due to the breaking of inversion symmetry between any two centrosymmetric phases. Sum frequency generation occurs when two laser beams are spatially and temporally overlapped on the surface. The resultant signal occurs at the sum of the infrared, ω_{IR}, and visible, ω_{Vis}, input frequencies:

$$\omega_{SF} = \omega_{IR} + \omega_{Vis} \tag{1}$$

SFG signal intensity, I_{SFG}, is mediated by the macroscopic hyperpolarizability tensor $\chi^{(2)}$. The macroscopic hyperpolarizability is the sum of resonant and nonresonant components. On dielectric surfaces the resonant portion dominates and is the one considered in this discussion.

$$I_{SFG} \propto |(\chi^{(2)}\mathbf{E}_1\mathbf{E}_2)|^2 \tag{2}$$

where $\mathbf{E}_1$and $\mathbf{E}_2$ are the electric fields of the input visible and infrared laser beams, respectively. The infrared frequency is scanned, and as it comes into resonance with a vibrational mode of the molecule, $\chi^{(2)}$ increases to a maximum, which results in a peak in the SFG spectrum.

As indicated in eq 2 the SFG intensity, I_{SFG}, is proportional to the square of the macroscopic hyperpolarizability. This macroscopic hyperpolarizibility, $\chi^{(2)}{}_{IJK}$, is related to the microscopic hyperpolarizibility, β_{IJK}, by

$$\chi^{(2)}{}_{IJK} = N\langle\beta_{IJK}\rangle \tag{3}$$

where N is the number of molecules contributing to the SFG signal, IJK refers to the surface fixed coordinate system, and $\langle\ \rangle$ indicates an ensemble average over the orientational distribution.

The molecular coordinates project onto the surface fixed axes as follows:

$$\beta_{IJK} = \sum U_{IJK:ijk}\beta_{ijk} \tag{4}$$

where $U_{IJK:ijk}$ is the Euler angle transformation matrix. Molecular orientation is deduced by determining the dominant molecular hyperpolarizability tensor elements, β_{ijk}, where ijk is the molecular coordinate system. Details of these transformations have been explicitly stated by others.[16−20]

Expansion of the nonlinear polarization equation indicates that resonanance enhancement occurs only if a specific mode

[⊗] Abstract published in *Advance ACS Abstracts,* May 15, 1997.

S1089-5647(96)03863-1 CCC: $14.00 © 1997 American Chemical Society

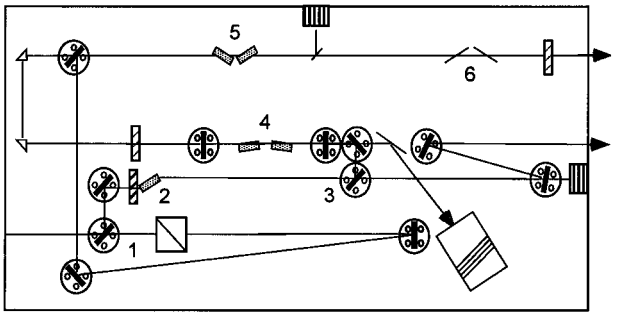

Figure 1. Optical parametric oscillator/amplifier (OPO/OPA) layout: 1 = 1064 nm beam splitter, 2 = KTP doubling crystal, 3 = 532 nm beam splitter, 4 = OPO, 5 = OPA, and 6 = ZnSe polarizer.

is both infrared and Raman active.[17]

$$\beta_{ijk} = \langle g|\alpha_{ij}|v\rangle\langle v|\mu_k|g\rangle \quad (5)$$

where β_{ijk} is the resonant molecular hyperpolarizability, α_{ij} is the Raman polarizability tensor, μ_k is the transition dipole operator, and g and v are the ground and excited vibrational states, respectively. SFG yields information on bonding via these vibrational resonances. Molecular orientation is determined by analyzing the signal intensity for different input and output polarization combinations.

Experimental Section

A nanosecond pulsed Nd:YAG and custom built OPO/OPA are used to perform sum frequency generation experiments at the air/liquid interface. The optical layout consists of a GCR 150 Nd:YAG laser (Spectra Physics, 700 mJ/pulse 1064 nm, ~9 ns pulse width, 10 Hz) pumping a KTP-based OPO/OPA (LaserVision[21]) continuously tunable from ~2600 to 4000 cm^{-1} with an energy of 1−5 mJ/pulse. Infrared bandwidth is ~4 cm^{-1} as determined with a CH_4(g) cell. The wavelength of the mid-infrared is calibrated with a CH_4(g) or HCl(g) cell.

The optical layout of the OPO/OPA is shown in Figure 1. The Nd:YAG fundamental is split with about 60% sent to the amplifier (OPA) for difference frequency generation (DFG). The remaining 1064 nm light is doubled in a KTP crystal to 532 nm. The 532 nm light is split with about 60% directed to the oscillator stage and the remainder sent to the sample for the SFG experiment. The oscillator contains two KTP crystals mounted on computer-controlled rotation stages counter-rotated to each other. This stage generates tunable idler/signal waves. Wavelength is controlled by angle tuning the crystals. The idler output is sent to the amplifier stage, which contains two, counter-rotated KTP crystals for DFG. The resulting mid-infrared radiation is tunable from 2700 to 4000 cm^{-1} with energies of 1−5 mJ/pulse. The residual pump beam is separated from the infrared beam with a 1064 nm reflector. The amplified idler beam is polarized 90° from the mid-infrared beam, and a ZnSe polarizer is used to separate them. Polarization and divergence of the infrared beam are controlled with a MgF_2 half-wave plate and 1000 mm, focal-length CaF_2 lens, respectively.

A diagram of the experimental setup is shown in Figure 2. The infrared beam is 1 mm diameter with an energy density of 50−200 mJ/cm^2, depending on the spectral region. The entire infrared line is enclosed in a dry N_2 purge to prevent intensity loss due to absorption by atmospheric water vapor. The infrared beam is incident on the surface at an angle of 46° from the normal, and the 532 nm light is incident on the surface at an angle of 52°. The 532 nm light is collimated with a telescope, and its power is controlled with a polarizer/half-wave plate combination. The 532 nm beam diameter is 2 mm, normal to

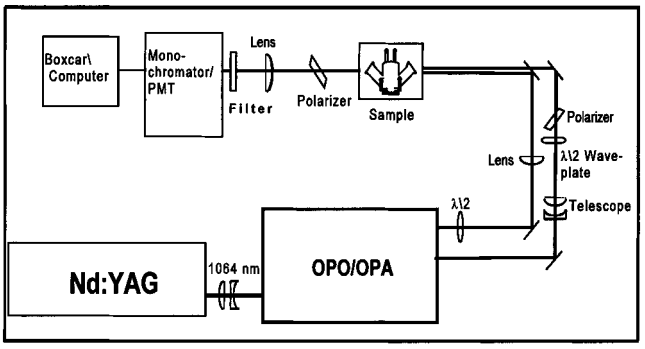

Figure 2. SFG optical layout. The fundamental of the Nd:YAG pumps a KTP-based OPO/OPA. This produces ~40 mJ/pulse of 532 nm light and 1−5 mJ/pulse of mid-infrared radiation. The 532 nm beam is expanded and collimated with a telescope, and the power is controlled with a polarizer/half-wave plate. The 532 nm beam is incident on the surface at an angle of 52°. The infrared beam divergence is controlled with a CaF_2 lens and is incident on the surface at 46°. The SF signal passes through a polarizer and is focused on the entrance slit of the monochromator.

the beam, with an energy density of ~200 mJ/cm^2. Care was taken to ensure that the energy was well below the nonlinear signal range for both the infrared and 532 nm beams. This is determined by performing power dependence experiments at the infrared resonances and then conducting the actual experiment where the signal has a linear dependence on input power.

The reflected sum frequency and the 532 nm beams are separated by an angle of 1°. The reflected 532 nm light is spatially filtered from the SFG. The sum frequency beam passes through a polarizer, a 450 nm, short-pass, interference filter and is focused onto the entrance slit of a 0.25 m, Jarrell-Ash monochromator. The sum frequency signal is collected with a PMT (Hamamatsu R4332), amplified with a ×10 amplifier, sent to a gated boxcar/averager (Stanford Research Systems, SR250), and collected by a computer for processing. Spectra are collected by averaging 1600 shots/point every 2 or 4 cm^{-1} depending on the spectral region. The spectra are corrected for the variation in infrared intensity by dividing by the average infrared intensity at each wavelength.

The reference procedure involves optimizing the input and output beam alignment to maximize the signal of the standard. The standard is the free OH of pure water for the hydroxyl region, while the CH_2(sym) of pure glycerol is the standard for the CH region. The standard and cell are removed, and the sample, in a matched cell, is put in its place. This ensures that alignment from spectrum to spectrum is consistent. The procedure is done before each spectrum. This method allows for compensation of variations in parameters such as beam overlap and laser intensity so that the spectra can be compared.

Glycerol (ACS grade >99%) are purchased from Aldrich Chemical and heated to about 50 °C under vacuum (80 mTorr) for several days before use to remove possible volatile components and water. All samples are handled under dry nitrogen to avoid contamination. The sample shows no significant impurities as determined by mass spectrometry. The sample is introduced into an all glass/Teflon vacuum tight cell with Teflon O-ring valves. The cell entrance window is CaF_2, and the exit window is quartz. The cell was cleaned with chromate/concentrated sulfuric acid solution and thoroughly rinsed and leached with 18 MΩ water. Spectra are collected at 0 °C, except pure glycerol, which was at room temperature. After more than a month of running the same sample, no changes were seen in the spectrum.

The purity of water is determined by an absence of signal in the 2800−3100 cm^{-1} region, indicating that possible contami-

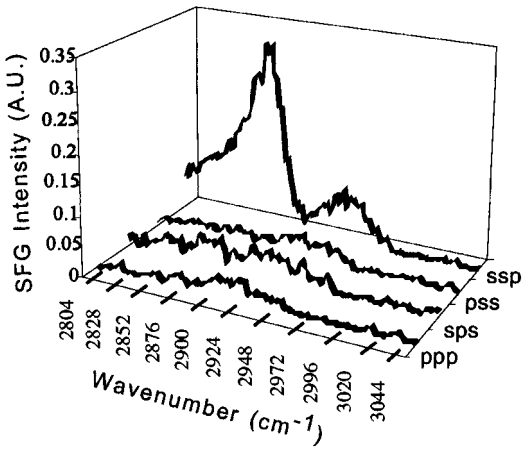

Figure 3. Summary of polarization combinations for pure glycerol sample. The notation ssp, for example, refers to s-polarized SF, s-polarized (532 nm) visible, and p-polarized infrared.

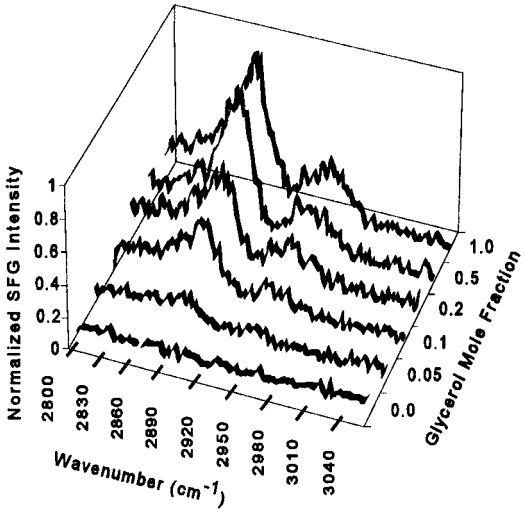

Figure 4. SFG spectra of the CH region of glycerol for various concentrations, ssp polarization combination.

nation due to surface active molecules is below our detection limit (Figure 3). This also validates our sample-handling procedure. SFG is a sensitive check for surface contamination.

Results

The SFG spectra of neat glycerol, for various polarization combinations, appear in Figure 3. This set of experiments demonstrates that only the ssp polarization combination has significant intensity (ssp refers to s-polarized SF, s-polarized (532 nm) visible, and p-polarized infrared). All further discussion will refer to this polarization combination. The spectra in Figure 4 have two significant peaks, a sharp resonance at 2880 cm^{-1} and a smaller peak at 2940 cm^{-1}. The peak at 2880 cm^{-1} is assigned to the CH_2 symmetric stretch, and at 2940 cm^{-1} to the asymmetric stretch. Figure 4 shows the CH region of glycerol for various glycerol mole fractions. Both symmetric and asymmetric modes decrease as water is added to glycerol. The detection limit for glycerol is between 0.05*x* and 0.01*x*. This is in the range of detection limits reported by others.[5,6] Spectra in Figure 5 show a decrease in free OH of water as a function of glycerol mole fraction. Above about 0.25*x* glycerol, free OH is below the detection limit. The signal level of the free OH in pure water is about 1/4 the intensity of the CH_2-(sym) peak in the spectrum of pure glycerol.

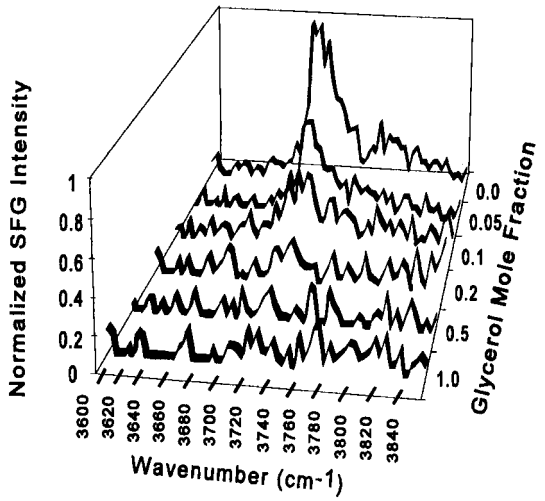

Figure 5. Free OH of water for various mole fractions of glycerol with ssp polarization combination.

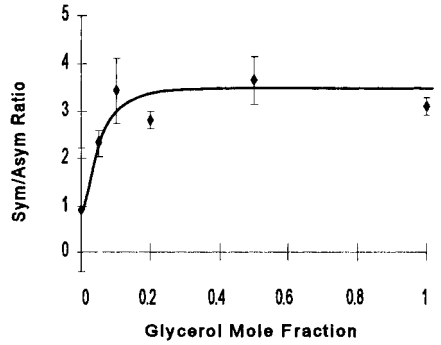

Figure 6. Ratio of CH_2(sym)symmetric/asymmetric modes of glycerol/water solutions. The solid line is a guide for the eye.

Discussion

The study of surface chemistry at liquid interfaces has not progressed to nearly the extent of that on solid surfaces. This is unfortunate since many important reactions occur at these surfaces. Prior to the last decade, little molecular detail could be obtained on these systems. However, details of the surfaces are beginning to reveal themselves with techniques such as SFG and molecular beam scattering.[22] This work reports on the surface vibrational spectra of glycerol and glycerol/water mixtures. These measurements, in combination with theoretical,[23] molecular beam surface scattering,[22] and classical measurements,[24] help to develop a molecular picture of vapor/liquid interfaces.

Constant Orientation. SFG intensity depends on both the number and orientation of surface molecules. If a molecule's orientation is constant, then $N \propto (I_{SFG})^{1/2}$. In this case $(I_{SFG})^{1/2}$ is plotted as a function of bulk mole fraction to determine surface concentration. For the CH_2 group on glycerol, the ratio of symmetric to asymmetric intensities is determined by the orientation of glycerol. This ratio, shown in Figure 6, does not change and therefore indicates approximately constant orientation of glycerol from 0.1*x* to 1.0*x*. This analysis assumes that solvation of glycerol does not significantly perturb the CH modes in either energy or oscillator strength. The assumption is supported by a lack of either wavelength shift or band shape change as glycerol is diluted. Since orientation does not change in the 0.1−1.0*x* glycerol range, the decrease of CH_2(sym) intensity is a measure of the decrease in the number of glycerol molecules on the surface.

Preliminary polarization analysis indicates that glycerol molecules are oriented with the carbon chain perpendicular to

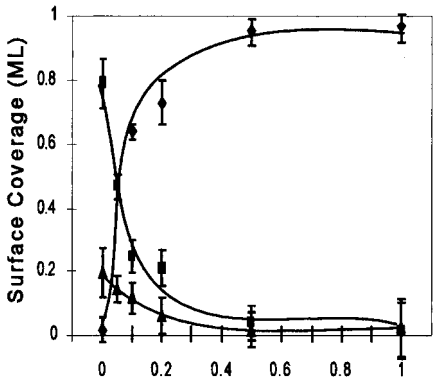

Figure 7. Surface coverage vs bulk mole fraction glycerol: ◆ = CH_2-(sym) of glycerol, ■ = hydrogen-bonded water, ▲ = free OH of water.

the surface plane. A more definitive assignment and orientation analysis will be presented in a forthcoming paper.[25]

Surface Partitioning of Glycerol. Glycerol and water are completely miscible, forming a nearly ideal solution. However, a plot of the surface coverage as a function of mole fraction glycerol, shown in Figure 7, reveals a somewhat surprising result: the surface of this completely miscible system is dominated by glycerol. This conclusion is arrived at as follows.

The number of molecules on the surface, N, is proportional to $(I_{SFG})^{1/2}$, assuming no orientation change as discussed above. Therefore, a plot of $(I_{SFG})^{1/2}$ as a function of bulk mole fraction glycerol indicates surface coverage relative to a monolayer (ML).

To calculate the surface mole fraction of glycerol, the following scheme is used. The SF signal at the neat glycerol surface is assigned a value of 1 ML glycerol. The fractional coverage (in number of molecules/cm^2) is determined by

$$N_s = \sqrt{I_{SFG}/I_{SFG,ML}}N_{ML} \tag{6}$$

where N_s is the number of molecules on the surface per cm^2, N_{ML} is the number of molecules/cm^2 in a monolayer, I_{SFG} and $I_{SFG,ML}$ are the sum frequency intensities measured at a specific concentration and a monolayer, respectively. On the basis of our orientation analysis and surface tension work by Chattoraj and Moulik,[24] a glycerol molecule occupies approximately 20Å^2, twice as much surface area as a water molecule, 10Å^2. Therefore, the monolayer signal from glycerol represents half as many molecules as the monolayer signal from water. Once the relative number of molecules of each kind on the surface is known, a surface mole fraction can be calculated.

$$x_s = \frac{N_{s,glycerol}}{N_{s,water} + N_{s,glycerol}} \tag{7}$$

Results for this determination are shown in Figure 8, which indicates that for all glycerol concentrations the surface is enriched in glycerol.

Free OH Glycerol. The structure of the glycerol/air interface is not obvious. Glycerol does not have a definite polar/nonpolar end as do *n*-alcohols or long-chain amphiphiles. Theoretical calculations seem to indicate the possibility of a free OH on the pure glycerol surface.[23] As the surface is approached from the vapor side, 40% of the time the first atom encountered is a hydroxyl hydrogen.[23] Gas phase Raman spectroscopy indicates that the free OH for glycerol is expected at ~3660 cm^{-1}.[26] However the spectrum of pure glycerol in Figure 5 shows no peaks in the 3450-3800 cm^{-1} region. Therefore, there are no free OH groups projecting out of the pure glycerol surface. Indeed, for all concentrations, the hydroxyl groups of glycerol

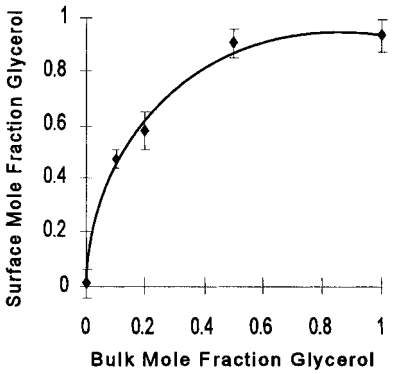

Figure 8. Surface mole fraction vs bulk mole fraction glycerol. The solid line is a guide for the eye.

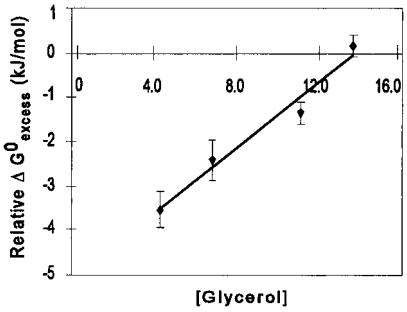

Figure 9. Free energy as a function of bulk number of moles of glycerol.

are never free. This observation and theoretical calculation seem to be contradictory, but they are not. Although the hydroxyl hydrogen may be the first atom encountered, it is not necessarily a free OH group.[27]

Molecular beam scattering experiments[22] determine that the surface of pure glycerol is rough and hydrophilic. Surface roughness allows for an irregular arrangement of glycerol molecules at the surface with some molecules sticking out higher or lower at the surface than others. This rough surface allows for more hydrogen bonding to take place than would be possible on a flat surface. Surface corrugation reconciles the SFG observation with theoretical calculation.

Glycerol/Water Mixtures. Glycerol partitions to the surface of glycerol water mixtures, which is seen in Figure 8. A simple equation can be written for this process.

$$\text{glycerol}_{bulk} \rightleftarrows \text{glycerol}_{surface} \tag{8}$$

Since the relative concentration of glycerol is known in both phases, free energy can be calculated for the process of moving a molecule from the bulk to the surface. This free energy is relative to that of the pure glycerol surface. The ΔG°_{excess} calculated here represents the extra or excess energy the system gains by partitioning glycerol to the solution interface. This is similar to calculating the chemical potential describing the driving force or escaping tendency of a component from one phase to another. Therefore, the ΔG°_{excess} for pure glycerol is zero, and a negative ΔG°_{excess} indicates that the surface mole fraction of glycerol exceeds that of the bulk. The surface excess free energy is given by

$$\Delta G^\circ_{excess} = -RT\ \ln(K), \quad \text{where } K = \frac{x_{glycerol,surface}}{x_{glycerol,bulk}} \tag{9}$$

Figure 9 shows the dependence of ΔG°_{excess} on glycerol mole fraction. The positive slope indicates there is a driving force for glycerol to move to the interfacial region as the solution is diluted.

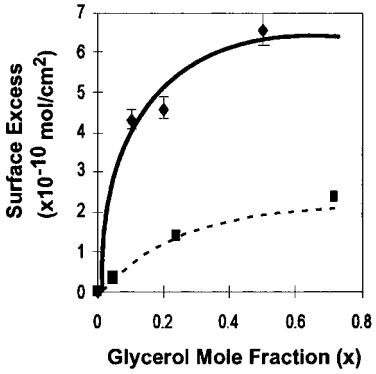

Figure 10. Surface excess vs bulk mole fraction glycerol: (···) surface tension data,[28] (—) SFG data.

TABLE 1: Surface Excess As Calculated by SFG Data and Surface Tension Data

bulk mole fraction glycerol	SFG excess (molecules/cm^2)	surface tension excess (molecules/cm^2)	surface tension (dyn/cm)
0.72		2.38×10^{-10}	64.66
0.5	6.56×10^{-10}		
0.24		1.40×10^{-10}	66.68
0.2	4.6×10^{-10}		
0.11		6.10×10^{-11}	68.42
0.1	4.32×10^{-10}		
0.047		3.60×10^{-11}	69.49
0	0	0	70.25

Surface tension[28] data are consistent with this result showing a decrease in surface free energy as glycerol is added to water and partitioning of glycerol to the surface.[24] Surface partitioning is indicated as a surface excess. Calculations of surface excess from surface tension data are accomplished with the help of the Gibbs equation,

$$\Gamma_G = \frac{-1}{RT}\frac{\partial\gamma}{\partial \ln c} \tag{10}$$

where Γ_G is the surface excess of glycerol in mol/cm^2, γ is surface tension, c is concentration, and RT are the gas constant and temperature, respectively. Results of the calculation are shown in Table 1 and Figure 10.

Surface excess has been shown to be related to the surface mole ratio relative to the bulk mole ratio,[24]

$$\Gamma_G = \frac{\Delta n_G}{A}\left[1 - \frac{x_G/x_W}{\Delta n_G/\Delta n_W}\right] = \frac{\Delta n_G}{A}(\Delta n_G/\Delta n_W - x_G/x_W)\frac{\Delta n_G}{\Delta n_W} \tag{11}$$

The surface excess, Γ_G, is calculated from eq 11, where Δn_G and Δn_W are the number of moles of glycerol and water, and x is the bulk mole fraction. A is the normalized area calculated by eq 12:

$$A = N_A(\Delta n_W \sigma_W + \Delta n_G \sigma_G) \tag{12}$$

where σ is the cross sectional area of water and glycerol, respectively. Equation 11 is also used to calculate surface excess from the SFG data. Results of this calculation are shown in Table 1.

SFG and surface tension measurements of excess are compared in Figure 10. SFG measurements differ by a factor of 3−6, with surface tension being consistently lower. This is due to SFG and surface tension measuring different depths of the surface region. SFG detects only the anisotropically ordered layer of the surface, while surface tension is a macroscopic measurement. In particular, SFG indicates surface excesses that are a large fraction of a monolayer. For example at 0.5x bulk mole fraction the surface concentration would be 1:1 glycerol/water if the surface mole fraction equaled the bulk mole fraction. However, the SFG measured surface mole ratio is approximately 9:1. Therefore the surface excess is eight glycerol molecules per water, or eight out of nine glycerol molecules are in excess. This is a large fraction of a monolayer.

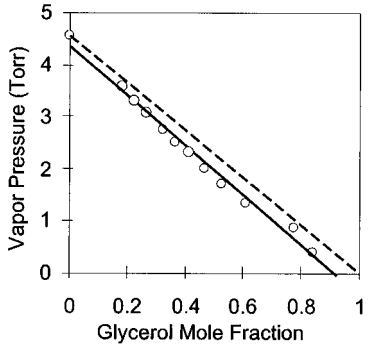

Figure 11. Vapor pressure of water vs mole fraction glycerol: (···) Raoult's law, (—) experimental.[28]

Water on Surface. Another view of the surface can be obtained by examining the gas/surface interactions. For example, at 0.5x glycerol, nearly all the vapor is composed of water (≪0.01% glycerol).[28] Under equilibrium conditions, water is constantly evaporating from and condensing on the surface. This could lead to a layer or (possibly a few) layers of water on the surface. Considering the high viscosity and low diffusion coefficient of glycerol, this view is reasonable. However, a few molecular layers of water on the surface would appear as an SFG spectrum of a water surface with a free OH peak. No such peak is detected in these experiments even when the water content approaches 0.75 bulk mole fraction water. This observation may be explained on the basis that the surface of the glycerol solution is a higher energy state for water than the bulk solution, resulting in a depletion of water at the surface.

The picture that emerges is that the surface layer does not reflect partitioning in either the vapor phase or bulk solution. The vapor pressure is a linear function of bulk mole fraction[28] and deviates only slightly from Raoult's law, also shown in Figure 11. Hence, despite the definite excess of glycerol molecules at the interface, the transport of water between the bulk phases has not been affected.

In summary these SFG results agree with the desiccating nature of glycerol. Water that lands on the surface is quickly drawn into the interior. Although a neat glycerol surface has no free OH groups for hydrogen bonding, dangling electron lone pairs can make the surface strongly hydrogen bonding. Below 0.25x glycerol (or >0.75x water) the surface contains free OH, which increase smoothly to a maximum number at pure water (∼25% of the surface).[3]

Conclusion

In this work, SFG is used to probe surface composition of glycerol water mixtures. Surface composition deviates significantly from that of the bulk. The surface is enriched in glycerol, and no free water OH is observed above 0.25x glycerol. Further, no free OH due to glycerol is observed at any concentration. There is a surface deficit of water despite the vapor being nearly 100% water, a result consistent with the surface partitioning of glycerol and the surface being a higher energy state for water.

Acknowledgment. We thank Prof. Ilan Benjamin and Prof. Gil Nathanson for helpful discussions. We are also very grateful

to Dean Guyer of LaserVision for his expert assistance in these experiments. Acknowledgment for partial support of this work is made to the National Science Foundation (Grant No. CHE-9208232), the U.S. Environmental Protection Agency (Award No. R-822453-01-0), and the Tufts University Center for Environmental Management. C.S. is supported by the NSF (CHE-9256871).

References and Notes

(1) Langmuir, I. *Colloidal Symposium Series*; The Chemical Catalog Company, New York, 1925.
(2) Adamson, A. W. *Physical Chemistry of Surfaces*, 5th ed.; John Wiley and Sons: New York, 1990.
(3) Du, Q.; Superfine, R.; Freysz, E.; Shen, Y. R. *Phys. Rev. Lett.* **1993**, *70*, 2313−2316.
(4) Shen, Y. R. *Nature* **1989**, *337*, 519.
(5) Wolfrum, K.; Graener, H.; Laubereau, A. *Chem. Phys. Lett.* **1993**, *213*, 41.
(6) Zhang, D.; Gutow, H.; Eisenthal, K. B.; Heinz, T. F. *J. Chem. Phys.* **1993**, *98*, 5099.
(7) Zhu, X. D.; Suhr, H.; Shen, Y. R. *Phys. Rev. B* **1987**, *35*, 3047.
(8) Superfine, R.; Huang, J. Y.; Shen, Y. R. *Opt. Lett.* **1990**, *15*, 1276.
(9) Superfine, R.; Huang, J. Y.; Shen, Y. R. *Chem. Phys. Lett.* **1990**, *172*, 303.
(10) Hunt, J. H.; Guyot-Sionnest, P.; Shen, Y. R. *Chem. Phys. Lett.* **1987**, *133*, 189.
(11) Huang, J.; Shen, Y. R. *Phys. Rev. A* **1994**, *49*, 3973.
(12) Guyot-Sionnest, P.; Superfine, R.; Hunt, J. H.; Shen, Y. R. *Chem. Phys. Lett.* **1988**, *144*, 1.
(13) Guyot-Sionnest, P.; Shen, Y. R. *Phys. Rev. B* **1987**, *35*, 4420.
(14) Du, Q.; Freysz, E.; Shen, R. *Science* **1994**, *264*, 826.
(15) Du, Q.; Freysz, E.; Shen, Y. R. *Phys. Rev. Lett.* **1994**, *72*, 238.
(16) Yamamoto, H.; Akamatsu, N.; Wada, A.; Hirose, C. *J. Electron Spectrosc. Relat. Phenom.* **1993**, *64/65*, 507.
(17) Hirose, C.; Akamatsu, N.; Domen, K. *J. Chem. Phys.* **1992**, *96*, 997−1004.
(18) Akamatsu, N.; Domen, K.; Hirose, C.; Yamamoto, H. *J. Phys. Chem.* **1993**, *97*, 10064.
(19) Akamatsu, N.; Domen, K.; Hirose, C. *Appl. Spectrosc.* **1992**, *46*, 1051−1102.
(20) Dick, B. *Chem. Phys.* **1985**, *96*, 199−215.
(21) Guyer, D. LaserVision, 11010 Northup Way Bellevue,WA.
(22) Saecker, M. E.; Nathanson, G. *J. Chem. Phys.* **1993**, *99*, 7056−7075.
(23) Benjamin, I.; Wilson, M.; Pohorille, A. *J. Chem. Phys.* **1994**, *100*, 6500.
(24) Chattoraj, D. K.; Moulik, S. P. *Ind. J. Chem.* **1977**, *15a*, 73.
(25) Baldelli, S.; Campbell, D. J.; Schnitzer, C.; Shultz, M. J. *J. Phys. Chem.*, submitted.
(26) Masson, M.; Royer, H.; Dupeyrat, R. *C. R. Acad. Sci. Ser B* **1972**, *274*, 62.
(27) Benjamin, I. Personal communication.
(28) Miner, C. S.; Dalton, N. N. *Glycerol*; Reinhold Publishing Corp.: New York, 1953.